

RESEARCH ARTICLE

Online Gaussian Process learning-based Model Predictive Control with Stability Guarantees

Michael Maiworm¹ | Daniel Limon² | Rolf Findeisen*¹¹Institute for Automation Engineering,
Otto-von-Guericke-University, Magdeburg,
Germany²Department of Systems Engineering and
Automation, Universidad de Sevilla,
Seville, Spain**Correspondence***R. Findeisen, Institute for Automation
Engineering, Otto-von-Guericke-University,
39106 Magdeburg, Germany. Email:
rolf.findeisen@ovgu.de**Summary**

Model predictive control provides high performance and safety in the form of constraint satisfaction. These properties however can be satisfied only if the underlying model used for prediction of the controlled process is of sufficient accuracy. One way to address this challenge is by data-driven and machine learning approaches, such as Gaussian processes, that allow to refine the model online during operation. We present a combination of a output feedback model predictive control scheme, which does not require full state information, and a Gaussian process prediction model that is capable of online learning. To this end the concept of evolving Gaussian processes is combined with recursively updating the posterior prediction. The presented approach guarantees input-to-state stability w.r.t. to the model-plant mismatch. Extensive simulation studies show that the Gaussian process prediction model can be successfully learned online. The resulting computational load can be significantly reduced via the combination of the recursive update procedure and limiting the number of training data points, while maintaining performance at a comparable level.

KEYWORDS:

predictive control, machine learning, gaussian processes, online learning, input-to-state stability, recursive updates

1 | INTRODUCTION

Model predictive control (MPC)¹ is naturally capable of dealing with multi-input multi-output systems and constraints on the input, state, and output, already in the design process. This has led to manifold scientific publications and practical applications.^{2,3} In terms of performance, MPC is often superior to other control approaches because it uses a prediction of the process under consideration, which allows to compute control actions based on future outcomes and allows to take preview information about references and disturbances into account. The model used for prediction plays a critical role in model predictive control. However, there is almost always a certain process-model error or model uncertainty present, or

the system might change over time, which limits its prediction quality. One way to deal with this situation is to resort to robust MPC schemes, such as, for instance, min-max MPC⁴, tube based MPC⁵, multi-scenario approaches^{6,7}, or stochastic approaches⁸ that take the uncertainty explicitly into account.

Models for prediction are traditionally obtained using first principle modeling based approaches. Unfortunately, it is sometimes very time consuming or even impossible to determine a reasonable model. Furthermore, if the underlying process or environmental conditions change during operation, a once determined model becomes less reliable and needs to be update/adapted. An alternative in these situations is to derive prediction models directly from measured data. The resulting models are often denoted as black or grey box models⁹ and can, in principle, be learned or refined during operation by including newly available data. Thereby, they are able to

account for changing process dynamics or a changing process environment. If necessary, combining data-driven with first principles models is also possible and often beneficial.^{10,11,12}

Although data-driven modeling is not a new field of research, it gained significant attention over the last years due to increasing computational power and the rise of various machine learning algorithms, such as neural networks, deep learning, or support vector machines. In this work we consider Gaussian process (GP) regression^{13,14}, which can be used to learn and model the underlying dynamics of the systems. The resulting Gaussian process can then be used as a prediction model within an MPC scheme.^{15,10,16,11,17,18} In comparison to other machine learning methods GPs do not only provide a prediction but also a prediction variance; an effective measure of the uncertainty of the learned model.

Though online learning (or adaptation) of a Gaussian process is highly desirable to account for time varying systems or changing environmental conditions, very few publications exist that combine MPC with online learning of GPs. One reason for this lies in the challenging learning process, which includes updates of the training data set and covariance matrix, recalculation of the covariance matrix inverse, and hyperparameter optimization in each time step. This requires computations that take often too long for most processes. Thus, when it comes to real world implementations, GPs are mostly trained/learned offline.^{19,17,20} Exceptions are the works by Ortmann et al²¹, where the system has a large time constant in the order of hours or Klenske et al¹⁶, which provides a hyperparameter optimization tailored to the specific application.

Another important aspect when combining Gaussian processes and model predictive control is stability, for which different approaches have been proposed. At first, stability was not enforced by design but instead, the GP posterior variance was included in the cost function of the optimal control problem to avoid steering the plant into regions where the model validity is questionable.^{22,23,24} Furthermore, one can perform a posteriori stability verification. For instance, Berkenkamp et al²⁵ proposed to learn the region of attraction of a given closed-loop system, whereas Vinogradskaya et al²⁶ calculate invariant sets for the validation of stability in a closed-loop with GP models. Another approach that can be found in the literature uses invariant *safe sets* and usually employs a two-layer control framework, where a safe controller is combined with a control policy that optimizes performance.^{27,28,29,30} Similarly, one can use set-based safety nets^{31,30}, like tube MPC schemes. Two different prediction models are used in parallel, where the first is a nominal model used to guarantee robust stability using tubes and the other can be a general learning-based model (e.g. a Gaussian process) used to optimize performance. In the work of Soloperto et al³² tube MPC is considered explicitly together with GPs. There

however, the GP model is also used for robust stability, which is why the stability guarantees are not deterministic but probabilistic. These approaches are based on the assumption of full state information, the use of an invariant terminal region, as well as a min-max tube based constraint.

This work is an extension of Maiworm et al¹⁸, where we combined a GP prediction model with an output feedback MPC scheme that does not require full state information nor terminal region. We showed under which conditions robust stability in the form of input-to-state stability w.r.t. the model error can be guaranteed. In comparison to the previous work, the main contributions of this work are:

- Online learning at minimal computational cost, which facilitates the possibility of deployment for fast processes. For this purpose, we employ a recursive formulation to update the GP prediction model online.
- Guaranteed robust stability for online learning. The result is thereby not confined to Gaussian processes but holds for general prediction models that are learned online and satisfy the presented conditions.
- The extension of the method such that it yields good performance with only limited prior process knowledge (e.g. lack of training data in important regions of the operation space). To this end we incorporate the concept of evolving GPs to facilitate online learning by means of adaptation of the training data set.^{33,14} We derive criteria that use the GP prediction error and the variance to determine which points to add to the training data set.
- Use of an analytic linearized GP model for the determination of the MPC terminal ingredients.

We denote the resulting control scheme as recursive GP model predictive control (rGP-MPC).

The paper is structured as follows: The considered problem setup is formulated in Section 2. The concept of Gaussian processes, together with the recursive formulation for online learning, is outlined in Section 3 and used for the formulation of the optimal control problem in Section 4. The same section also contains the stability results. Section 5 presents simulation results with focus on the online learning of the Gaussian process, before Section 6 concludes the paper.

Notation Vectors and matrices are set using bold variables. For a given set $\mathcal{Y} \subset \mathbb{R}^p$ and a point $\mathbf{y} \in \mathbb{R}^p$, the distance of the point to the set is defined as $d(\mathbf{y}, \mathcal{Y}) = \inf_{\mathbf{z} \in \mathcal{Y}} \|\mathbf{z} - \mathbf{y}\|_\infty$, where $\|\cdot\|_\infty$ is the infinity norm. If not stated otherwise, $\|\cdot\|$ denotes the Euclidian vector norm. A function $\alpha : \mathbb{R}_{\geq 0} \rightarrow \mathbb{R}_{\geq 0}$ is a \mathcal{K} -function if $\alpha(0) = 0$ and it is strictly increasing. A function $\alpha : \mathbb{R}_{\geq 0} \rightarrow \mathbb{R}_{\geq 0}$ is a \mathcal{K}_∞ -function if it is a \mathcal{K} -function and unbounded. A function $\beta : \mathbb{R}_{\geq 0} \times \mathbb{R}_{\geq 0} \rightarrow \mathbb{R}_{\geq 0}$

is a \mathcal{KL} -function if $\beta(s, t)$ is \mathcal{K}_∞ in s for any value of t and $\lim_{t \rightarrow \infty} \beta(s, t) = 0, \forall s \geq 0$.

2 | PROBLEM FORMULATION

We consider nonlinear discrete time systems that can be represented by a nonlinear autoregressive model with exogenous input (NARX)

$$y_{k+1} = f(\mathbf{x}_k, u_k, \mathbf{e}_k) + \epsilon \quad (1a)$$

$$\text{s.t. } u_k \in \mathcal{U}, \quad (1b)$$

where k denotes the discrete time index, $u_k \in \mathbb{R}$ the input, $y_k \in \mathbb{R}$ the output, $\mathbf{e}_k \in \mathcal{E}$ is a signal that represents model error¹, and $\mathbf{x}_k \in \mathbb{R}^{n_x}$ is the NARX state vector

$$\mathbf{x}_k = [y_k \ \dots \ y_{k-m_y} \ u_{k-1} \ \dots \ u_{k-m_u}]^\top \quad (2)$$

that consists of the current and past outputs and inputs, where m_y, m_u determine the NARX model order $n_x = m_y + m_u + 1$.² The output is corrupted by white Gaussian noise $\epsilon \sim \mathcal{N}(0, \sigma_n^2)$ with zero mean and noise variance σ_n^2 . Additionally, the input is restricted by hard constraints \mathcal{U} and the output by soft constraints \mathcal{Y} , i.e., the output should stay in a certain region $y_k \in \mathcal{Y} \subseteq \mathbb{R}$, if possible.

The considered control objective is a set-point stabilization and optimal set-point change; we want to steer the system from an initial equilibrium $(\mathbf{x}_{\text{ini}}, u_{\text{ini}})$ to a target reference equilibrium $(\mathbf{x}_{\text{ref}}, u_{\text{ref}})$, while satisfying the constraints and stabilize the system at the set-point. To this end we employ model predictive control, which requires a model of the process (1) that is capable of predicting future output values with sufficient accuracy. We will outline an approach to learn the model from measured input-output data using a Gaussian process, which is capable of online learning during operation based on newly available data. This results in a GP-based NARX prediction model.

3 | GAUSSIAN PROCESSES

We first review the basics of Gaussian process regression, derive the GP prediction gradient required for the MPC formulation, and present a recursive GP (rGP) formulation that is based on the concept of evolving GPs, which facilitates the generation of a NARX prediction model capable of adapting to changing conditions. To reduce the online computational cost, we combine this concept with a recursive update of the involved Cholesky decomposition.

3.1 | GP Basics

A Gaussian process is a *collection of random variables, any finite number of which have a joint Gaussian distribution*.¹³

It generalizes the Gaussian probability distribution to distributions over functions and can therefore be used to model/approximate functions that can be used to capture dynamic systems.¹⁴ Gaussian processes can be utilized for purely data derived models or they can be combined with other, for instance, deterministic models.^{11,12,10,34,35,27,25,28,32}

For regression, GPs are employed to derive or approximate maps of the form $z = f(\mathbf{v}) + \epsilon$ with input \mathbf{v} , output z , where $f(\cdot)$ is the underlying but unknown *latent* function. The output is assumed to be corrupted by white Gaussian noise $\epsilon \sim \mathcal{N}(0, \sigma_n^2)$ with zero mean and noise variance σ_n^2 . The objective is to infer the function $f(\cdot)$ using measured input-output data (\mathbf{v}, z) with a Gaussian process $g(\mathbf{w})$ with input $\mathbf{w} \in \mathbb{R}^{n_w}$, called *regressor*. In the present case (1a), we have $z_k = y_{k+1}$ and $f(\mathbf{v}) = f(\mathbf{x}_k, u_k, \mathbf{e}_k)$. The regressor of the GP will be $\mathbf{w}_k = (\mathbf{x}_k, u_k) \in \mathbb{R}^{n_w}$ with regressor order $n_w = n_x + 1$. For the sake of brevity we omit the dependence on the discrete time step k in the remainder of this section whenever possible.

The first required ingredient is a GP prior distribution

$$g(\mathbf{w}) \sim \mathcal{GP}(m(\mathbf{w}), k(\mathbf{w}, \mathbf{w}')) , \quad (3)$$

which is specified via the mean function

$$m(\mathbf{w}) = \mathbb{E}[g(\mathbf{w})]$$

and the covariance function³

$$\begin{aligned} k(\mathbf{w}, \mathbf{w}') &= \text{cov}[g(\mathbf{w}), g(\mathbf{w}')] \\ &= \mathbb{E}[(g(\mathbf{w}) - m(\mathbf{w}))(g(\mathbf{w}') - m(\mathbf{w}'))] , \end{aligned}$$

with $\mathbf{w}, \mathbf{w}' \in \mathbb{R}^{n_w}$ and $\mathbb{E}[\cdot]$ denoting the expected value. The mean and covariance function together with a set of so called hyperparameters θ , which we detail further below, fully specify the GP.

The GP prior is then trained/learned using a set of n measured input-output data points, where the input data set is $\mathbf{w} = [\mathbf{w}_1 \dots \mathbf{w}_n]^\top \in \mathbb{R}^{n \times n_w}$ and the output data set $\mathbf{z} = [z_1 \dots z_n]^\top \in \mathbb{R}^{n \times 1}$. The combined data set $\mathcal{D} = \{\mathbf{w}, \mathbf{z}\}$ that is available at time step k is denoted as training data set and is used to infer the posterior distribution

$$g(\mathbf{w}|\mathcal{D}) \sim \mathcal{GP}(m_+(\mathbf{w}|\mathcal{D}), \sigma_+^2(\mathbf{w}|\mathcal{D})) ,$$

which is also a Gaussian process with posterior mean $m_+(\mathbf{w}|\mathcal{D})$ and variance $\sigma_+^2(\mathbf{w}|\mathcal{D})$ given by

$$m_+(\mathbf{w}|\mathcal{D}) = m(\mathbf{w}) + k(\mathbf{w}, \mathbf{w}) \mathbf{K}^{-1}(\mathbf{z} - m(\mathbf{w})) \quad (4a)$$

$$\sigma_+^2(\mathbf{w}|\mathcal{D}) = k(\mathbf{w}, \mathbf{w}) - k(\mathbf{w}, \mathbf{w}) \mathbf{K}^{-1} k(\mathbf{w}, \mathbf{w}) \quad (4b)$$

¹More properties on the signal \mathbf{e}_k and the set \mathcal{E} are given in Section 4.4.

²Without loss of generality we consider in this work systems with one input. In that case, the NARX state space dimension n_x equals the NARX model order. For more than one input the state space dimension would be larger than the model order.

³The covariance function is also denoted as *kernel*.

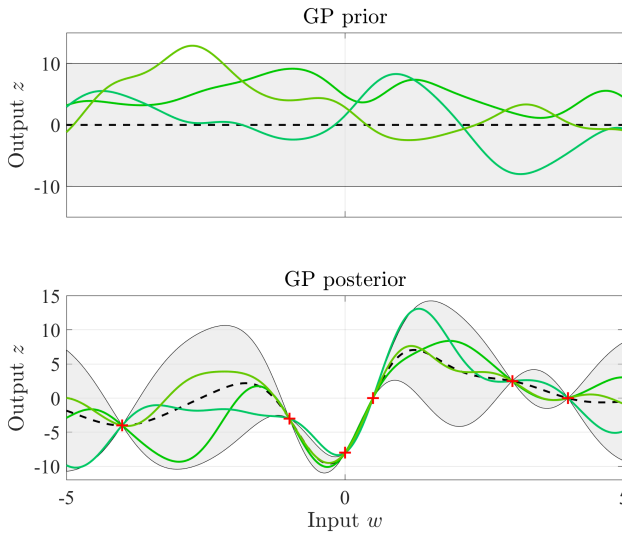


FIGURE 1 Gaussian process inference: The top figure depicts a GP prior distribution with the dashed black line denoting the mean function $m(\mathbf{w})$ and the green lines denoting random function realizations drawn from the prior distribution. The grey shaded area is the 95 % (twice the standard deviation) confidence interval computed via $k(\mathbf{w}, \mathbf{w}')$. When data points \mathcal{D} are added (bottom figure, red crosses), the GP posterior with $m_+(\mathbf{w}|\mathcal{D})$ and $\sigma_+^2(\mathbf{w}|\mathcal{D})$ is inferred from this data.

with $m(\mathbf{w}) = [m(\mathbf{w}_1) \dots m(\mathbf{w}_n)]^\top \in \mathbb{R}^{n \times 1}$, $k(\mathbf{w}, \mathbf{w}) = [k(\mathbf{w}, \mathbf{w}_1) \dots k(\mathbf{w}, \mathbf{w}_n)] \in \mathbb{R}^{1 \times n}$, $k(\mathbf{w}, \mathbf{w}) = k(\mathbf{w}, \mathbf{w})^\top$, and $\mathbf{K} = k(\mathbf{w}, \mathbf{w}) = [k(\mathbf{w}_i, \mathbf{w}_j)] \in \mathbb{R}^{n \times n}$.

Note that realizations of the posterior can yield infinitely many function outcomes but as it is conditioned on the training data points, it rejects all possible functions that do not go through or nearby (if $\sigma_n^2 \neq 0$) these points (Fig. 1).

The posterior mean function (4a) is the desired estimator of the unknown output latent function $f(\mathbf{x}_k, u_k, \mathbf{e}_k)$ in (1a), which we highlight by defining

$$\hat{y}_{k+1} = \hat{z} := m_+(\mathbf{w}_k | \mathcal{D}_k), \quad (5)$$

where the hat notation ($\hat{\cdot}$) denotes an estimated quantity.

The key ingredients for a Gaussian process to yield a sensible model are the prior mean and covariance function. Both depend generally on a set of hyperparameters θ , i.e., $m(\mathbf{w}|\theta)$ and $k(\mathbf{w}, \mathbf{w}'|\theta)$. Very often just a constant zero prior mean $m(\mathbf{w}|\theta) = c = 0$ is used.^{15,36,37} However, other choices include, for instance, the use of a deterministic base model $\mathbf{x}_{k+1} = f(\mathbf{x}_k, u_k)$ as the prior mean function.^{10,38} In the case of dynamic systems, the most often used covariance function is

the *squared exponential covariance function*⁴ with automatic relevance determination

$$k(\mathbf{w}_i, \mathbf{w}_j | \theta) = \sigma_f^2 \exp\left(-\frac{1}{2}(\mathbf{w}_i - \mathbf{w}_j)^\top \Lambda (\mathbf{w}_i - \mathbf{w}_j)\right) + \sigma_n^2 \delta_{ij}, \quad (6)$$

where $\mathbf{w}_i, \mathbf{w}_j \in \mathbb{R}^{n_w}$, $\Lambda = \text{diag}(l_1, \dots, l_{n_w})$, $\theta = \{\sigma_f^2, \Lambda\}$ are the covariance hyperparameters, onto which the measurement noise σ_n^2 is added via the Kronecker delta δ_{ij} . The minimal required number of regressors n_w can be determined through optimization of the length scale parameters l in Λ .^{40,41} Other choices include, for instance, the combination of (6) with a linear kernel.^{40,42}

A common approach to determine the hyperparameters θ , given a training data set $\mathcal{D} = \{\mathbf{w}, \mathbf{z}\}$, is to maximize the log marginal likelihood¹³

$$\log(p(\mathbf{z}|\mathbf{w}, \theta)) = -\frac{1}{2}\mathbf{z}^\top \mathbf{K}^{-1} \mathbf{z} - \frac{1}{2} \log |\mathbf{K}| - \frac{n}{2} \log(2\pi). \quad (7)$$

A main advantage of GPs is that (4b) naturally provides a quantification of the model uncertainty in the form of its variance. On the other hand, the involved computations in (4a) and (4b) scale with $\mathcal{O}(n^3)$, where n is the number of training data points. This severely limits the application of GP models for fast processes, where small sampling times are required. Especially in the case of relatively large training data sets with several hundreds or thousands of data points. If hyperparameter optimization is needed, this drawback becomes even more pronounced.

3.2 | Evolving GPs

In order to efficiently refine the GP model online we want to update the training data set \mathcal{D}_k possibly at each time step k during operation. To this end we resort to the concept of so called *evolving GPs*.^{33,14} They can be used if the underlying system to be modeled by a GP is time varying and needs to be adjusted/learned online, or if the training data is only available for certain sections of the operating region and one wants to expand operation beyond these sections. The concept describes basically GPs whose training data set \mathcal{D} is updated online using some type of information criterion. Different criteria can be used to select new data points to be added and already existing points to be removed if necessary.

The general idea is to include an incoming data point to the training data set only if it contributes new valuable information, which can be defined in different ways and depends on the application of the GP. Possible options are the use of the information gain, entropy difference, or the expected likelihood.^{43,44} We employ the GP as a prediction model in MPC

⁴Note that the squared exponential covariance function is sometimes also denoted as *Gaussian radial basis function*. Especially in the field of neural networks.³⁹

and are therefore particularly interested in how accurate the current model is able to predict the output value at the next time step. Hence, given a new data point (\mathbf{w}_k, z_k) , if the prediction error

$$e_{k+1}^p := y_{k+1} - \hat{y}_{k+1} = z_k - m_+(\mathbf{w}_k | \mathcal{D}_k) \quad (8)$$

is larger than a pre-specified threshold \bar{e}^p , the data point is included in the training data set \mathcal{D}_k because the current posterior model is not able to predict the output with the specified accuracy. If it is smaller but the resulting posterior variance $\sigma_+^2(\mathbf{w} | \mathcal{D}_k)$ is larger than a pre-specified threshold $\bar{\sigma}^2$, the data point is also included because the current posterior model is not sufficiently confident in its prediction. This approach allows to include only data points that are relevant to attain a certain prediction quality and effectively minimizes the necessary number of data points in \mathcal{D}_k . This becomes especially important for long operation times and many encountered data points with new information during operation.

As the available computational power is always limited and depending on the concrete system, this can require the limitation of the maximum number of points in \mathcal{D}_k by a constant $M \in \mathbb{N}$. If this limit is reached despite inclusion criteria like the ones detailed above, data points have to be removed to maintain the size of \mathcal{D}_k . Again, different criteria can be employed to determine which data point shall be deleted. For instance, the point in the training data set with the lowest benefit for the model quality (e.g. the data point that is most accurately predicted under the current posterior) can be deleted. Another and more simple approach that we propose to employ in this work is to delete the oldest point contained in \mathcal{D}_k .

Remark 1. The concept of evolving GPs, in particular the data handling approach explained above, automatically leads to a training data set \mathcal{D} that captures only the system dynamics in an (evolving) subregion of the whole operating region. This means also that information about the dynamics of already visited regions can be lost when moving towards other regions and have to be regained when visited again. This can be counteracted using multiple GPs for different regions or GP blending.

Remark 2. Besides the presented update approach we require an additional update rule for theoretical reasons that is presented in Sec. 4.4.

3.3 | Cholesky Decomposition

The squared exponential covariance function (6) and other smooth covariance functions lead to a poor conditioned covariance matrix \mathbf{K} .^{45,46} This results in numerical problems when computing the inverse \mathbf{K}^{-1} with computational cost $\mathcal{O}(n^3)$,

as required for (4a), (4b), or (7). These problems become even worse if (4a) and (4b) are nested within an optimization procedure like MPC.

One way to alleviate this problem is by adding an additional noise or *jitter* term⁴⁵ to the diagonal of the covariance matrix. The most effective approach however is to avoid the numerical instabilities that arise in the explicit computation of the matrix inverse by performing the required computations using the Cholesky decomposition, which is numerically more stable.

Given a system of linear equations $\mathbf{Ax} = \mathbf{b}$ with a symmetric positive matrix \mathbf{A} , we denote the solution by $\mathbf{x} = \mathbf{A}^{-1}\mathbf{b} := \mathbf{A} \setminus \mathbf{b}$. The Cholesky decomposition of \mathbf{A} is $\mathbf{A} = \mathbf{R}^\top \mathbf{R}$, where $\mathbf{R} = \text{chol}(\mathbf{A})$ is an upper triangular matrix that is called the *Cholesky factor*. It can be used to obtain the solution via $\mathbf{x} = \mathbf{R} \setminus (\mathbf{R}^\top \setminus \mathbf{b})$.

In order to use the Cholesky factor to solve (4a) and (4b), we define

$$\begin{aligned} \boldsymbol{\alpha} &:= \mathbf{K}^{-1}(\mathbf{z} - m(\mathbf{w})) \\ \boldsymbol{\beta} &:= \mathbf{K}^{-1}k(\mathbf{w}, \mathbf{w}), \end{aligned}$$

which can then be computed with the Cholesky decomposition $\mathbf{K} = \mathbf{R}^\top \mathbf{R}$ via

$$\begin{aligned} \boldsymbol{\alpha} &= \mathbf{R} \setminus (\mathbf{R}^\top \setminus (\mathbf{z} - m(\mathbf{w}))) \\ \boldsymbol{\beta} &= \mathbf{R} \setminus (\mathbf{R}^\top \setminus k(\mathbf{w}, \mathbf{w})). \end{aligned} \quad (9)$$

The computational cost of computing \mathbf{R} is $\mathcal{O}(n^3/6)$ and the cost of computing $\boldsymbol{\alpha}$ and $\boldsymbol{\beta}$ is $\mathcal{O}(n^2)$.¹³ In order to further reduce these costs, we show in the following how to update the Cholesky factor \mathbf{R} recursively.

3.3.1 | Recursive Update

If the training data set \mathcal{D}_k does not change, the Cholesky decomposition $\mathbf{K} = \mathbf{R}^\top \mathbf{R}$ and the computation of $\boldsymbol{\alpha}$ have to be performed only once at the beginning, whereas $\boldsymbol{\beta}$ has to be recomputed for every new test point \mathbf{w} . If \mathcal{D}_k changes, i.e., with each inclusion or removal of a data point, the covariance matrix \mathbf{K} has to be updated for an appropriate evaluation of the GP posterior. If a data point is included, a row and column have to be added to \mathbf{K} . If a data point is removed, the respective row and column associated with this point have to be removed. These changes require in principle a full recalculation of the Cholesky factor \mathbf{R} , which is the most expensive computation. To reduce this computational load we propose to recalculate the Cholesky factor recursively, taking advantage of the available factor of the previous step. We base our approach on the work by Osborne⁴⁶.

Regarding the case of including a new data point, consider the covariance matrix \mathbf{K} , represented in block form as

$$\begin{bmatrix} \mathbf{K}_{11} & \mathbf{K}_{13} \\ \mathbf{K}_{13}^T & \mathbf{K}_{33} \end{bmatrix}$$

and its Cholesky factor

$$\begin{bmatrix} \mathbf{R}_{11} & \mathbf{R}_{13} \\ 0 & \mathbf{R}_{33} \end{bmatrix}.$$

Now, given an updated covariance matrix

$$\begin{bmatrix} \mathbf{K}_{11} & \mathbf{K}_{12} & \mathbf{K}_{13} \\ \mathbf{K}_{12}^T & \mathbf{K}_{22} & \mathbf{K}_{23} \\ \mathbf{K}_{13}^T & \mathbf{K}_{23}^T & \mathbf{K}_{33} \end{bmatrix}$$

that differs from the previous by insertion of a new row and column, the updated Cholesky factor

$$\begin{bmatrix} \mathbf{S}_{11} & \mathbf{S}_{12} & \mathbf{S}_{13} \\ 0 & \mathbf{S}_{22} & \mathbf{S}_{23} \\ 0 & 0 & \mathbf{S}_{33} \end{bmatrix}.$$

can be computed via

$$\begin{aligned} \mathbf{S}_{11} &= \mathbf{R}_{11} & \mathbf{S}_{22} &= \text{chol}(\mathbf{K}_{22} - \mathbf{S}_{12}^T \mathbf{S}_{12}) \\ \mathbf{S}_{12} &= \mathbf{R}_{11}^T \setminus \mathbf{K}_{12} & \mathbf{S}_{23} &= \mathbf{S}_{22}^T \setminus (\mathbf{K}_{23} - \mathbf{S}_{12}^T \mathbf{S}_{13}) \\ \mathbf{S}_{13} &= \mathbf{R}_{13} & \mathbf{S}_{33} &= \text{chol}(\mathbf{R}_{33}^T \mathbf{R}_{33} - \mathbf{S}_{23}^T \mathbf{S}_{23}) . \end{aligned} \quad (10)$$

On the other hand, if the current covariance matrix in block form

$$\begin{bmatrix} \mathbf{K}_{11} & \mathbf{K}_{12} & \mathbf{K}_{13} \\ \mathbf{K}_{12}^T & \mathbf{K}_{22} & \mathbf{K}_{23} \\ \mathbf{K}_{13}^T & \mathbf{K}_{23}^T & \mathbf{K}_{33} \end{bmatrix}$$

with Cholesky factor

$$\begin{bmatrix} \mathbf{R}_{11} & \mathbf{R}_{12} & \mathbf{R}_{13} \\ 0 & \mathbf{R}_{22} & \mathbf{R}_{23} \\ 0 & 0 & \mathbf{R}_{33} \end{bmatrix}$$

is reduced by one row and column, such that we obtain

$$\begin{bmatrix} \mathbf{K}_{11} & \mathbf{K}_{13} \\ \mathbf{K}_{13}^T & \mathbf{K}_{33} \end{bmatrix},$$

the downdated Cholesky factor

$$\begin{bmatrix} \mathbf{S}_{11} & \mathbf{S}_{13} \\ 0 & \mathbf{S}_{33} \end{bmatrix}$$

can be computed via

$$\begin{aligned} \mathbf{S}_{11} &= \mathbf{R}_{11} \\ \mathbf{S}_{13} &= \mathbf{R}_{13} \\ \mathbf{S}_{33} &= \text{chol}(\mathbf{R}_{23}^T \mathbf{R}_{23} + \mathbf{R}_{33}^T \mathbf{R}_{33}) . \end{aligned} \quad (11)$$

Due to the recursive nature, both in the data inclusion approach and the Cholesky decomposition, we denote the resulting Gaussian process as recursive GP (rGP). The algorithm including the most important steps of the resulting rGP-MPC formulation is presented in Algorithm 1.

Remark 3. This approach can only be applied if the hyper-parameters θ do not change because otherwise every single element of \mathbf{K} changes.

Remark 4. There exists also an approach based on the partitioned block inverse to recursively update directly the covariance matrix inverse \mathbf{K}^{-1} . Presumably for the numerical issues outlined in Sec. 3.3, this approach has never been used in combination with MPC. It has however in the signal processing literature, where it is strongly connected to the concept of *kernel recursive least-squares*.^{47,48}

4 | GAUSSIAN PROCESS BASED OUTPUT MODEL PREDICTIVE CONTROL

In this section we present the output model predictive control formulation, based on the rGP NARX model for prediction. We highlight the necessary ingredients, derive a bound for the model error that depends on the GP prediction error, and show under which conditions stability can be guaranteed even if the GP model changes online.

4.1 | Prediction Model

In Section 4.4 we establish input-to-state stability (ISS) for the considered system, which is defined using the evolution of the state and not the output. For this reason we reformulate (1a) in terms of the state \mathbf{x}_k into $\mathbf{x}_{k+1} = F(\mathbf{x}_k, \mathbf{u}_k, \mathbf{e}_k)$. We start by setting $k := k + 1$ in (2) and arrive at

$$\mathbf{x}_{k+1} = [y_{k+1}, y_k, \dots, y_{k+1-m_y}, \mathbf{u}_k, \dots, \mathbf{u}_{k+1-m_u}] .$$

Since the next output y_{k+1} is computed by (1a) we obtain the NARX state model

$$\begin{aligned} \mathbf{x}_{k+1} &= F(\mathbf{x}_k, \mathbf{u}_k, \mathbf{e}_k) \\ &= [f(\mathbf{x}_k, \mathbf{u}_k, \mathbf{e}_k) + \epsilon, y_k, \dots, y_{k+1-m_y}, \mathbf{u}_k, \dots, \mathbf{u}_{k+1-m_u}] \end{aligned} \quad (12)$$

with output equation $y_k = \mathbf{c}^T \mathbf{x}_k$ and $\mathbf{c}^T = [1 \ 0 \ \dots \ 0]$.

The NARX state model without error term and noise is denoted as the nominal NARX state model

$$\hat{\mathbf{x}}_{k+1} = [\hat{f}(\hat{\mathbf{x}}_k, \mathbf{u}_k), \hat{y}_k, \dots, \hat{y}_{k+1-m_y}, \mathbf{u}_k, \dots, \mathbf{u}_{k+1-m_u}] ,$$

where $\hat{f}(\hat{\mathbf{x}}_k, \mathbf{u}_k) \triangleq f(\mathbf{x}_k, \mathbf{u}_k, 0)$ is the nominal model of (1a), which we define to be the GP predictor (5), i.e.,

$$\hat{f}(\hat{\mathbf{x}}_k, \mathbf{u}_k) := m_+(\mathbf{w}_k | \mathcal{D}_k) = \hat{y}_{k+1}$$

with $\mathbf{w}_k = (\hat{\mathbf{x}}_k, \mathbf{u}_k)$. The final nominal/prediction model to be used in the MPC becomes

$$\begin{aligned} \hat{\mathbf{x}}_{k+1} &= \hat{F}(\hat{\mathbf{x}}_k, \mathbf{u}_k | \mathcal{D}_k) \\ &= [m_+(\mathbf{w}_k | \mathcal{D}_k), \hat{y}_k, \dots, \hat{y}_{k+1-m_y}, \mathbf{u}_k, \dots, \mathbf{u}_{k+1-m_u}] . \end{aligned} \quad (13)$$

4.2 | Optimal Control Problem

Using the prediction model (13), we consider at each time step k the optimal control problem

$$\begin{aligned} \min_{\hat{\mathbf{u}}_{k|k}} & V_N(\mathbf{x}_k, \hat{\mathbf{u}}_{k|k}) \\ \text{s.t. } & \forall i \in \mathcal{I}_{0:N-1} : \\ & \hat{\mathbf{x}}_{k+i|k} = \hat{F}(\hat{\mathbf{x}}_{k+i|k}, \hat{\mathbf{u}}_{k+i|k} | \mathcal{D}_k) \quad (14) \\ & \hat{\mathbf{x}}_{k|k} = \mathbf{x}_k \\ & \hat{\mathbf{u}}_{k+i|k} \in \mathcal{U}. \end{aligned}$$

The input sequence to be optimized is denoted by $\hat{\mathbf{u}}_{k|k} = \{\hat{u}_{k|k}, \dots, \hat{u}_{k+N-1|k}\}$, N is the prediction horizon, and \mathbf{x}_k is the initial condition of the measured NARX state (2). The cost function is

$$V_N(\mathbf{x}_k, \hat{\mathbf{u}}_{k|k}) = \sum_{i=0}^{N-1} \ell(\hat{\mathbf{x}}_{k+i|k}, \hat{\mathbf{u}}_{k+i|k}) + \lambda V_f(\hat{\mathbf{x}}_{k+N|k} - \mathbf{x}_{\text{ref}}),$$

where $V_f(\cdot)$ is the terminal cost function, $\lambda \geq 1$ a design parameter and associated to it is a terminal control law $\kappa_f(\cdot)$ that is important both in the computation of $V_f(\cdot)$ and to establish stability. The employed positive stage cost is given by

$$\ell(\hat{\mathbf{x}}_k, \hat{\mathbf{u}}_k) = \ell_s(\hat{\mathbf{x}}_k - \mathbf{x}_{\text{ref}}, \hat{\mathbf{u}}_k - u_{\text{ref}}) + \ell_b(\hat{y}_k),$$

where $\ell_s(\cdot)$ penalizes input and state deviations from the reference equilibrium and $\ell_b(\cdot)$ is a barrier function that accounts for the soft output constraints. It is defined by

$$\ell_b(\hat{y}_k) \geq \alpha_b(d(\hat{y}_k, \mathcal{Y})),$$

which satisfies $\ell_b(\hat{y}_k) = 0, \forall \hat{y}_k \in \mathcal{Y}$ and where $\alpha_b(\cdot)$ is a \mathcal{K} -function and $d(\cdot)$ the distance function as defined in Section 1.

The optimal solution of (14) is denoted by $\hat{\mathbf{u}}_{k|k}^*$ and its first element $\hat{u}_{k|k}^*$ is applied to the process, i.e., $u_k = \kappa_{\text{MPC}}(\mathbf{x}_k | \mathcal{D}_k) = \hat{u}_{k|k}^*$. Note that the implicitly defined control law κ_{MPC} is time-varying, as well as the optimal cost function $V_N^*(\mathbf{x}_k | \mathcal{D}_k) = V_N(\mathbf{x}_k, \hat{\mathbf{u}}_{k|k}^* | \mathcal{D}_k)$, also denoted as *value function*, because they depend on the changing prediction model associated with \mathcal{D}_k .

Note that (14) does not include any explicit terminal region constraint.

4.3 | Posterior Mean Gradient

The optimal control problem (14) requires terminal ingredients, which we base on a linearized version of the prediction model in Section 5. To this end we need the gradient of the GP posterior mean function

$$\nabla m_+(\mathbf{w}) = \frac{\partial m_+(\mathbf{w})}{\partial \mathbf{w}} = \left[\frac{\partial m_+(\mathbf{w}_1)}{\partial \mathbf{w}_1} \dots \frac{\partial m_+(\mathbf{w}_{n_w})}{\partial \mathbf{w}_{n_w}} \right]^\top$$

w.r.t. to its regressor $\mathbf{w} = [\mathbf{w}_1, \dots, \mathbf{w}_{n_w}]$, where we omit the dependence on the training data \mathcal{D} for the sake of brevity.

Assuming a constant prior mean in (4a) we obtain

$$\nabla m_+(\mathbf{w}) = \frac{\partial k(\mathbf{w}, \mathbf{w})}{\partial \mathbf{w}} \mathbf{K}^{-1} (\mathbf{z} - m(\mathbf{w}))$$

with

$$\frac{\partial k(\mathbf{w}, \mathbf{w})}{\partial \mathbf{w}} = \left[\frac{\partial k(\mathbf{w}, \mathbf{w}_1)}{\partial \mathbf{w}} \dots \frac{\partial k(\mathbf{w}, \mathbf{w}_n)}{\partial \mathbf{w}} \right],$$

where $\mathbf{w}_1, \dots, \mathbf{w}_n$ is the corresponding regressor of each of the n measured training data points in \mathcal{D} .

For the covariance function (6), we obtain

$$\frac{\partial k(\mathbf{w}, \mathbf{w}')}{\partial \mathbf{w}} = k^*(\mathbf{w}, \mathbf{w}') \Lambda(\mathbf{w}' - \mathbf{w}),$$

where $k^*(\mathbf{w}, \mathbf{w}')$ is (6) without the noise term, i.e., $\sigma_n^2 = 0$.

4.4 | Stability

We establish stability through a suitable chosen terminal cost function $V_f(\cdot)$ and terminal control law $\kappa_f(\cdot)$. The optimal control problem (14) does not require a terminal region because V_f is weighted by a factor $\lambda \geq 1$, as proposed by Limon et al⁴⁹. We consider stability first for the nominal case, i.e., when the prediction/nominal model (13) and the true system (12) are exactly the same. Afterwards, we consider the case when they are different and establish robust stability in the form of input-to-state stability assuming a bounded error signal \mathbf{e}_k .

Definition 1 (Input-to-state Stability). The closed-loop system $\mathbf{x}_{k+1} = F(\mathbf{x}_k, \kappa_{\text{MPC}}(\mathbf{x}_k | \mathcal{D}_k), \mathbf{e}_k)$ is input-to-state stable (ISS) if there exist a \mathcal{KL} -function $\beta(\cdot)$ and a \mathcal{K} -function $\gamma(\cdot)$ such that

$$\|\hat{\mathbf{x}}_k\| \leq \beta(\|\mathbf{x}_0\|, k) + \gamma \left(\max_{k \geq 0} \|\mathbf{e}_k\| \right) \quad (15)$$

holds for all initial states \mathbf{x}_0 , disturbances \mathbf{e}_k , and for all k .

The ISS property comprises the two effects of nominal stability and uniformly bounded influence of uncertainty in a single condition. It implies asymptotic stability of the undisturbed (nominal) system (with $\mathbf{e}_k \equiv 0$) and a bounded effect of the uncertainty on the state evolution. Furthermore, if the error signal \mathbf{e}_k fades, the uncertain system asymptotically converges to the equilibrium. We therefore establish nominal stability first and robust stability in the ISS sense afterwards.

4.4.1 | Nominal Stability

In the following let the current deviation from the reference point and the deviation at the next time step be $\tilde{\mathbf{x}} = \mathbf{x} - \mathbf{x}_{\text{ref}}$ and $\tilde{\mathbf{x}}^+ = \mathbf{x}^+ - \mathbf{x}_{\text{ref}}$.

Assumption 1. Assume that

1. the stage cost function $\ell(\mathbf{x}, \mathbf{u})$ is positive definite, i.e., $\ell(\mathbf{x}_{\text{ref}}, \mathbf{u}_{\text{ref}}) = 0$ and there exists a \mathcal{K}_∞ -function $\alpha(\cdot)$ such that $\ell(\tilde{\mathbf{x}}, \mathbf{u}) \geq \alpha(\|\tilde{\mathbf{x}}\|)$ for all $\mathbf{u} \in \mathcal{U}$, and

2. there exists a terminal control law $\kappa_f(\cdot)$ and let $V_f(\cdot)$ be a control Lyapunov function, such that the conditions

$$\alpha_1(\|\tilde{x}\|) \leq V_f(\tilde{x}) \leq \alpha_2(\|\tilde{x}\|)$$

and

$$V_f(\tilde{x}^+) \leq V_f(\tilde{x}) - \ell(\tilde{x}, \kappa_f(\tilde{x}) - u_{\text{ref}})$$

hold for all $\tilde{x} \in \Gamma_v = \{\tilde{x} \in \mathbb{R}^{n_x} : V_f(\tilde{x}) \leq v\}$ with $v > 0$, $\tilde{x}^+ = \hat{F}(\tilde{x}, \kappa_f(\tilde{x}) + u_{\text{ref}} | \mathcal{D}_k)$, and where $\alpha_1(\cdot)$ and $\alpha_2(\cdot)$ are \mathcal{K}_∞ -functions. The constant v is chosen such that for all $\tilde{x} \in \Gamma_v$ we get $c^\top \tilde{x} \in \mathcal{Y}$.

Assumption 1 can be addressed if we have a local description of the model and its uncertainty (e.g. a linear model with additive uncertainty) at the target equilibrium. For instance, using a GP model at the target or a deterministic estimator, such as Kinky inference, which can be derived from suitable local experimental data and standard identification procedures.⁵⁰

Assumption 2. Let \mathcal{D}_k be the training data set at time k and \mathcal{D}_{k+1} the one that will be used at time $k+1$. Let \mathcal{S}_{k+1} be the data point candidate to be added to \mathcal{D}_k and define $\mathcal{D}'_{k+1} = \mathcal{D}_k \cup \mathcal{S}_{k+1}$. To update \mathcal{D}_k the following rule is used:

If $V_N^*(\mathbf{x}_k | \mathcal{D}'_{k+1}) \leq V_N^*(\mathbf{x}_k | \mathcal{D}_k)$

$$\mathcal{D}_{k+1} \leftarrow \mathcal{D}'_{k+1}$$

else

$$\mathcal{D}_{k+1} \leftarrow \mathcal{D}_k$$

end

Hence, at \mathbf{x}_k the optimal control problem is solved with \mathcal{D}_k and the resulting $u_k = \kappa_{\text{MPC}}(\mathbf{x}_k | \mathcal{D}_k) = \hat{u}_{k|k}^*$ is applied to the system. If the next data point \mathbf{x}_{k+1} is a candidate for updating the GP, the previous optimal cost is recomputed using the updated GP. If the cost does not increase the GP update becomes effective. Hence, the update rule in Assumption 2 is executed additionally after the data selection process presented in Section 3.2. This is also reflected in Algorithm 1.

Theorem 1 (Nominal stability). Let $\kappa_{\text{MPC}}(\mathbf{x}_k | \mathcal{D}_k)$ be the predictive controller derived from the optimal control problem (14) satisfying Assumptions 1 and 2. Then $\forall \lambda \geq 1$, there exists a region $\mathcal{X}_N(\lambda)$ such that $\forall \mathbf{x} \in \mathcal{X}_N(\lambda)$, the nominal closed-loop system $\mathbf{x}_{k+1} = \hat{F}(\mathbf{x}_k, \kappa_{\text{MPC}}(\mathbf{x}_k | \mathcal{D}_k))$ is asymptotically stable. The size of the set $\mathcal{X}_N(\lambda)$ increases with λ .

Proof. Let $\hat{\mathbf{x}}_{k|k}^* = \{\hat{\mathbf{x}}_{k|k}^*, \hat{\mathbf{x}}_{k+1|k}^*, \dots, \hat{\mathbf{x}}_{k+N|k}^*\}$ be the predicted state sequence that results from applying the optimal input sequence $\hat{u}_{k|k}^*$. Then we can write the optimal cost for initial condition $\mathbf{x}_k = \hat{\mathbf{x}}_{k|k}^*$ also as $V_N^*(\mathbf{x}_k | \mathcal{D}_k) = V_N(\mathbf{x}_k, \hat{u}_{k|k}^* | \mathcal{D}_k) = V_N(\hat{\mathbf{x}}_{k|k}^*, \hat{u}_{k|k}^* | \mathcal{D}_k)$. Let furthermore $\hat{\mathbf{x}}_{k+1|k}^* = \{\hat{\mathbf{x}}_{k+1|k}^*, \dots, \hat{\mathbf{x}}_{k+N|k}^*\}$ and $\hat{u}_{k+1|k}^* = \{\hat{u}_{k+1|k}^*, \dots, \hat{u}_{k+N-1|k}^*\}$ be the respective sequences that start at $k+1$ computed at time k .

By Assumption 1 we have that the stage and terminal cost are positive definite. Hence, the cost function $V_N(\mathbf{x}_k, \hat{u}_{k|k}^*)$ is positive definite. Furthermore we also obtain

$$V_N(\hat{\mathbf{x}}_{k+1|k}^*, \hat{u}_{k+1|k}^* | \mathcal{D}_{k+1}) \leq V_N(\hat{\mathbf{x}}_{k|k}^*, \hat{u}_{k|k}^* | \mathcal{D}_{k+1}) - \ell(\mathbf{x}_k, u_k)$$

by Assumption 1, which is a well known result in standard MPC (for the derivation see, for instance, Rawlings and Mayne¹ or Rakovic et al⁵¹).

Due to Assumption 2 we have

$$\begin{aligned} & V_N(\hat{\mathbf{x}}_{k|k}^*, \hat{u}_{k|k}^* | \mathcal{D}_{k+1}) - \ell(\mathbf{x}_k, u_k) \\ & \leq V_N(\hat{\mathbf{x}}_{k|k}^*, \hat{u}_{k|k}^* | \mathcal{D}_k) - \ell(\mathbf{x}_k, u_k). \end{aligned}$$

Combining the previous two equations we obtain

$$V_N(\hat{\mathbf{x}}_{k+1|k}^*, \hat{u}_{k+1|k}^* | \mathcal{D}_{k+1}) \leq V_N(\hat{\mathbf{x}}_{k|k}^*, \hat{u}_{k|k}^* | \mathcal{D}_k) - \ell(\mathbf{x}_k, u_k).$$

Thus, the value function is decreasing even if the prediction model changes. Hence the value function is a Lyapunov function. Then Theorem 3 of Limon et al⁴⁹ guarantees that $\forall \lambda \geq 1$, there exists a region $\mathcal{X}_N(\lambda)$ such that $\forall \mathbf{x} \in \mathcal{X}_N(\lambda)$, the nominal closed-loop system $\mathbf{x}_{k+1} = \hat{F}(\mathbf{x}_k, \kappa_{\text{MPC}}(\mathbf{x}_k | \mathcal{D}_k))$ is asymptotically stable. The size of the set $\mathcal{X}_N(\lambda)$ increases with λ . \square

4.4.2 | Robust Stability

Based on Theorem 1 we show that the real process controlled by the proposed predictive controller is input-to-state stable w.r.t. the error signal \mathbf{e}_k .

Assumption 3. Assume that the error signal $\mathbf{e}_k \in \mathcal{E} \subset \mathbb{R}^{n_x}$, where \mathcal{E} is a compact set, resembles the process-model error between the true system and the GP prediction model, i.e., $\mathbf{e}_k := \mathbf{x}_k - \hat{\mathbf{x}}_k$, and assume furthermore that \mathbf{e}_k is bounded with $\|\mathbf{e}_k\| \leq \mu$.

Theorem 2 (Input-to-state Stability). Let $\kappa_{\text{MPC}}(\mathbf{x}_k | \mathcal{D}_k)$ be the predictive controller derived from optimal control problem (14) satisfying Assumptions 1 and 2. Furthermore, let Assumption 3 be fulfilled. If one of the two conditions

1. The stage cost function $\ell(\cdot, \cdot)$ and the terminal cost function $V_f(\cdot)$ are uniformly continuous in $\mathcal{X}_N(\lambda)$.
2. The nominal closed-loop $\hat{F}(\mathbf{x}_k, \kappa_{\text{MPC}}(\mathbf{x}_k))$ is uniformly continuous in \mathbf{x}_k for all $\mathbf{x}_k \in \mathcal{X}_N(\lambda)$.

hold, the closed-loop system $\mathbf{x}_{k+1} = F(\mathbf{x}_k, \kappa_{\text{MPC}}(\mathbf{x}_k | \mathcal{D}_k), \mathbf{e}_k)$ is ISS in a robust invariant set $\Omega \subseteq \mathcal{X}_N(\lambda)$ for a sufficiently small bound μ of the uncertainties. The smaller μ , the larger Ω .

⁵Note that Theorem 3 of Limon et al⁴⁹ is stated the other way round, i.e., for each region $\mathcal{X}_N(\lambda)$ and for all $\mathbf{x}_k \in \mathcal{X}_N(\lambda)$, there exists a $\lambda \geq 1$ such that the nominal closed-loop system is asymptotically stable at \mathbf{x}_{ref} .

Proof. The satisfaction of Assumptions 1 and 2 lead to asymptotic stability in the absence of uncertainty, guaranteed by Theorem 1. The remainder of the proof is a reformulation of Theorem 4 in Limon et al⁵².

1. If the first condition of Theorem 2 is satisfied, then uniform continuity of the cost function is guaranteed by Proposition 1 (condition C1) in Limon et al⁵², i.e., there exists a \mathcal{K}_∞ -function $\sigma(\cdot)$ such that

$$V_N(\mathbf{x}_{k+1}, \hat{\mathbf{u}}_{k+1|k}^* | \mathcal{D}_k) - V_N(\hat{\mathbf{x}}_{k+1|k}^*, \hat{\mathbf{u}}_{k+1|k}^* | \mathcal{D}_k) \leq \sigma(\|\mathbf{e}_k\|).$$

Then Theorem 4 in Limon et al⁵² holds. Note that in case of uncertainty we have in general $V_N(\mathbf{x}_{k+1}, \hat{\mathbf{u}}_{k+1|k}^* | \mathcal{D}_k) \neq V_N(\hat{\mathbf{x}}_{k+1|k}^*, \hat{\mathbf{u}}_{k+1|k}^* | \mathcal{D}_k)$ because $\mathbf{x}_{k+1} \neq \hat{\mathbf{x}}_{k+1|k}^*$.

2. If Assumption 3 and the second condition of Theorem 2 are satisfied, then Theorem 4 in Limon et al⁵² holds directly.

Satisfaction of Theorem 4 in Limon et al⁵² guarantees in combination with Theorem 1 above that the closed-loop system $\mathbf{x}_{k+1} = F(\mathbf{x}_k, \kappa_{\text{MPC}}(\mathbf{x}_k | \mathcal{D}_k), \mathbf{e}_k)$ is ISS. Furthermore, if $\|\mathbf{e}_k\| < \mu$, for a sufficiently small μ , the optimal control problem is recursively feasible in a robust invariant set $\Omega \subseteq \mathcal{X}_N(\lambda)$. \square

Remark 5. Theorems 1 and 2 hold for general process-model errors \mathbf{e}_k independent of the concrete structure of the state \mathbf{x}_k (here a NARX state). They furthermore hold for general prediction models $\hat{F}(\mathbf{x}_k, u_k | \mathcal{D}_k)$ that are updated online, i.e., the stability guarantees are not confined to the use of GP prediction models in model predictive control.

A sufficient condition in Theorem 2 is that the nominal model $\hat{F}(\mathbf{x}_k, u_k)$ is uniformly continuous. In the case of Gaussian processes this can be guaranteed by the following proposition.

Proposition 1 (GP Uniform Continuity¹⁸). The nominal model (13) is uniformly continuous if $\hat{f}(\mathbf{x}_k, u_k) = m_+(\mathbf{w}_k)$ is uniformly continuous. Since the prior mean $m(\mathbf{w}_k)$ is added to $m_+(\mathbf{w}_k)$, the prior mean has to be uniformly continuous⁶. Then, one way to ensure that $m^+(\mathbf{w})$ is uniformly continuous, is to employ continuously differentiable kernels (e.g. the squared exponential covariance function, the Matérn class covariance function with appropriate hyperparameters, or the rational quadratic covariance function). In that case the process is mean square differentiable^{53,13}, i.e., the posterior mean function is differentiable and therefore also uniformly continuous⁷.

Corollary 1. According to Assumption 3, the process-model error \mathbf{e}_k is bounded by μ . For the case that only outputs are

contained in \mathbf{x}_k we have⁸

$$\mathbf{e}_k = \mathbf{x}_k - \hat{\mathbf{x}}_k = \begin{bmatrix} y_k \\ y_{k-1} \\ \vdots \end{bmatrix} - \begin{bmatrix} \hat{y}_k \\ \hat{y}_{k-1} \\ \vdots \end{bmatrix} = \begin{bmatrix} e_k^p \\ e_{k-1}^p \\ \vdots \end{bmatrix}.$$

If the prediction error e^p is bounded throughout operation by \bar{e}^p , we can compute an estimate for μ via

$$\|\mathbf{e}_k\| \leq \sqrt{(\bar{e}^p)^2 + (\bar{e}^p)^2 + \dots} = \sqrt{n_x \cdot (\bar{e}^p)^2} = \bar{e}^p \sqrt{n_x} =: \mu.$$

According to Theorem 2 for all $\|\mathbf{e}_k\| < \mu$, the smaller $\|\mathbf{e}_k\|$, the larger Ω . Thus, the objective is to minimize $\|\mathbf{e}_k\|$, which by Corollary 1 translates to the minimization of the prediction error e^p . This in turn depends on the designer's choices regarding the particular employed GP model and the involved tuning parameters. For more detailed considerations regarding boundedness of Gaussian processes, see the works of Nicolao and Pillonetto⁵⁴ and Pillonetto and Chiuso⁵⁵.

5 | SIMULATIONS

In this section we provide simulation results for the presented rGP-MPC scheme. To this end we use a continuous stirred-tank reactor as a simulation case study. We present the model equations, the training data set generation, and the terminal ingredients for the MPC based on the linearized GP posterior mean function. The closed-loop simulations involve investigations regarding the tuning parameters of the rGP-MPC, the influence of different initial training data sets, as well as comparisons with other MPC controllers.

5.1 | Continuous Stirred-tank Reactor

In a continuous stirred-tank reactor (CSTR) a substrate A is converted into product B .⁵⁶ The reaction $A \rightarrow B$ can be described by the following set of differential equations

$$\dot{C}_A(t) = \frac{q_0}{V} (C_{A\text{f}} - C_A(t)) - k_0 \exp\left(\frac{-E}{RT(t)}\right) C_A(t) \quad (16a)$$

$$\begin{aligned} \dot{T}(t) &= \frac{q_0}{V} (T_{\text{f}} - T(t)) - \frac{\Delta H_{\text{r}} k_0}{\rho C_p} \exp\left(\frac{-E}{RT(t)}\right) C_A(t) \\ &\quad + \frac{U A}{V \rho C_p} (T_{\text{c}}(t) - T(t)) \end{aligned} \quad (16b)$$

$$\dot{T}_{\text{c}}(t) = \frac{T_{\text{r}}(t) - T_{\text{c}}(t)}{\tau}, \quad (16c)$$

where the coolant temperature reference T_{r} (K) is the input to the reactor and the concentration C_A (mol/l) the output, i.e., $u = T_{\text{r}}$ and $y = C_A$. The tank and coolant temperature are T and T_{c} , respectively. The model parameters are given in Tab. 1.

⁶The prior mean is usually specified by the user and often set to zero. Thus uniform continuity of $m(\mathbf{w})$ is not an issue.

⁷Continuous differentiability is a stronger assumption than uniform continuity.

⁸The current input u_k is never part of the NARX state vector \mathbf{x}_k , only previous inputs can be included if desired.

5.2 | Training Data Set

The plant (16) is used to generate a raw data set \mathcal{D}_{raw} (Fig. 2). Each data point (z_i, \mathbf{w}_i) consists of values of $(y_{k+1}, y_k, \dots, y_{k-m_y}, u_k, \dots, u_{k-m_u})$, where $z = y_{k+1}$ is going to be the GP output and $\mathbf{w} = (y_k, \dots, y_{k-m_y}, u_k, \dots, u_{k-m_u})$ its corresponding regressor. Based on this data, we generate the three training data sets \mathcal{D}_0 , \mathcal{D}_{ref} , and $\mathcal{D}_{\text{comb}}$, which are in the following used for comparative simulations. The set \mathcal{D}_0 is a local subset around the initial equilibrium $y_0 = C_A = 0.6 \text{ mol/l}$. The associated input is $u_0 = T_r = 353.5 \text{ K}$. The set \mathcal{D}_{ref} is a local subset around the target reference equilibrium $y_{\text{ref}} = C_A = 0.439 \text{ mol/l}$ with associated input $u_{\text{ref}} = T_r = 356 \text{ K}$. The set $\mathcal{D}_{\text{comb}} = \mathcal{D}_0 \cup \mathcal{D}_{\text{ref}}$ is the union of the two sets.

The sets \mathcal{D}_0 and \mathcal{D}_{ref} are generated by selecting first all points $z = y_{k+1}$ (and their corresponding \mathbf{w}) that are located within a local neighborhood of the respective equilibrium and second, by reducing the number of points via exclusion of those that add only little information. For a given data point (z_i, \mathbf{w}_i) , all following $(z_j, \mathbf{w}_j), j > i$, are removed, for which $\|\mathbf{w}_i - \mathbf{w}_j\| < \bar{w}$ with a chosen threshold \bar{w} . As a result, the sets are less dense but still contain enough informative data points. The thresholds for \mathcal{D}_0 and \mathcal{D}_{ref} are chosen such that both sets contain approximately 40 data points.

Remark 6. All input and output values are given in the original units of the system (16). However, it is beneficial for the modeling process with the GP to normalize the input-output data to the interval $[0, 1]$.

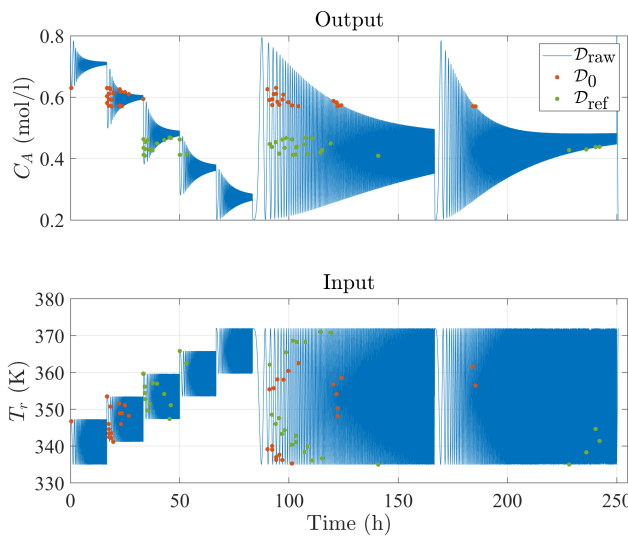


FIGURE 2 Training data sets: The raw data set \mathcal{D}_{raw} was generated by chirp signals on the input. The sets \mathcal{D}_0 and \mathcal{D}_{ref} are local neighborhoods of the initial equilibrium (u_0, y_0) and the reference equilibrium $(u_{\text{ref}}, y_{\text{ref}})$.

5.3 | GP Prediction Model

For the GP prior we employ a constant mean function with constant c and the covariance function (6) with regressor $\mathbf{w} = [y_k, y_{k-1}, y_{k-2}, u_k]$ and according to (1a), the NARX state is $\mathbf{x}_k = [y_k, y_{k-1}, y_{k-2}]$. The hyperparameters are $\theta = \{c, l_1, l_2, l_3, l_4, \sigma_f^2\}$ and are computed offline via maximization of (7) for each of the three data sets \mathcal{D}_0 , \mathcal{D}_{ref} , and $\mathcal{D}_{\text{comb}}$. We obtain three sets of hyperparameters respectively (Tab. 2) and with that three different GP prediction models that use the same prior but different training data sets and hyperparameters. The cross validation results of these different GP models are shown in Fig. 3, where we select test points throughout the regions of the respective training data sets. Test points are chosen such that they are not part of \mathcal{D}_0 , \mathcal{D}_{ref} , or $\mathcal{D}_{\text{comb}}$. As can be seen, appropriate GP predictions are achieved with prediction error $e^p < \bar{e}^p = 0.02 \text{ mol/l}$ and posterior standard deviation $\sigma < \bar{\sigma}^2 = 6 \cdot 10^{-3} \text{ mol/l}$ for all three GPs.

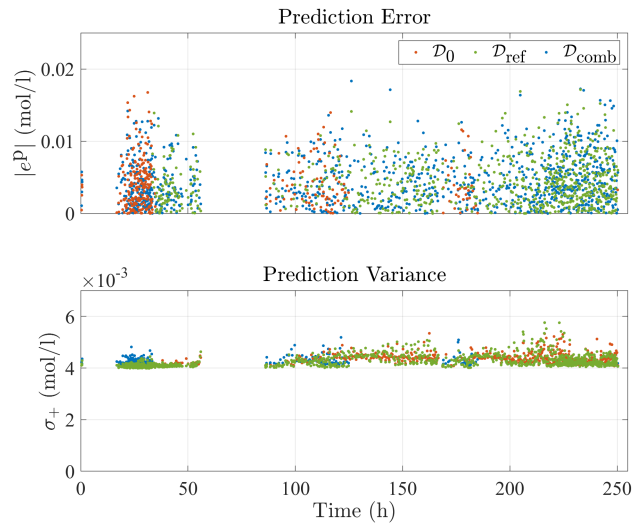


FIGURE 3 Cross validation results: In the top, the prediction error e^p (8) is depicted. In the bottom, the posterior standard deviation $\sigma(\mathbf{w}) = \sqrt{\sigma_f^2(\mathbf{w})}$.

5.4 | Optimal Control Problem

The continuous model (16) is discretized with Euler's method and a sampling time of $T_s = 0.5 \text{ min}$. The input constraints are $\mathcal{U} = \{335 \text{ K} \leq T_r \leq 372 \text{ K}\}$, the output constraints $\mathcal{Y} = \{0.35 \text{ mol/L} \leq C_A \leq 0.65 \text{ mol/l}\}$. We add measurement noise $\epsilon \sim \mathcal{N}(0, \sigma_n^2)$ to the output data with $\sigma_n^2 = 0.004^2$.

The employed quadratic stage cost is given by

$$\ell_s(\mathbf{x}_k, u_k) = \|\mathbf{x}_k - \mathbf{x}_{\text{ref}}\|_Q^2 + \|u_k - u_{\text{ref}}\|_R^2$$

with $\mathbf{Q} = \text{diag}(100, 0, 0)$, and $R = 5$. The barrier function to account for the soft output constraints is

$$\ell_b(y_k) = \xi(1 - \exp(-d(y_k, \mathcal{Y})/\delta))$$

with $\xi = 100$ and $\delta = 1$.

5.5 | Terminal Ingredients

The terminal controller $\kappa_f(\cdot)$ and cost function $V_f(\cdot)$ can be determined in any possible way, as long as the assumptions in Section 4.4 are satisfied. We choose the terminal controller as $\kappa_f(\mathbf{x}) = \mathbf{k}^\top(\mathbf{x} - \mathbf{x}_{\text{ref}}) + u_{\text{ref}}$ and the terminal cost function as $V_f(\mathbf{x}) = \|\mathbf{x} - \mathbf{x}_{\text{ref}}\|_P^2$, where \mathbf{k}^\top and \mathbf{P} are computed via the linearization of the prediction model (13) with the GP model based on \mathcal{D}_{ref} .

The linearization of the nominal NARX model $\mathbf{x}_{k+1} = \hat{F}(\mathbf{x}_k, u_k)$ with $\mathbf{x}_k = [y_k, y_{k-1}, y_{k-2}]$ takes the form

$$\begin{bmatrix} y_{k+1} \\ y_k \\ y_{k-1} \end{bmatrix} = \begin{bmatrix} a_{11} & a_{12} & a_{13} \\ 1 & 0 & 0 \\ 0 & 1 & 0 \end{bmatrix} \begin{bmatrix} y_k \\ y_{k-1} \\ y_{k-2} \end{bmatrix} + \begin{bmatrix} b_1 \\ 0 \\ 0 \end{bmatrix} u_k.$$

Since the next output is computed using the GP, i.e., $y_{k+1} = m_+(\mathbf{w}_k)$, the parameters $[a_{11}, a_{12}, a_{13}, b_1]$ can be determined using the posterior mean gradient derived in Sec. 4.3. In particular we have $[a_{11}, a_{12}, a_{13}, b_1] = \nabla m_+(\mathbf{w}_{\text{ref}})^\top$ with $\mathbf{w}_{\text{ref}} = [y_{\text{ref}}, y_{\text{ref}}, y_{\text{ref}}, u_{\text{ref}}]$.

The resulting linear model becomes

$$\mathbf{x}_{k+1} = \begin{bmatrix} 8.39 & 5.25 & 2.37 \\ 1 & 0 & 0 \\ 0 & 1 & 0 \end{bmatrix} \mathbf{x}_k + \begin{bmatrix} -12.1 \\ 0 \\ 0 \end{bmatrix} u_k. \quad (17)$$

Remark 7. Note that (17) depends on the employed GP and therefore on all its ingredients, i.e., hyperparameters, training data, etc..

The feedback vector \mathbf{k}^\top and terminal cost matrix \mathbf{P} are computed from the solution of the linear-quadratic regulator (LQR), using the linear model (17) and the weights \mathbf{Q} and R , yielding

$$\begin{aligned} \mathbf{P} &= \begin{bmatrix} 114 & 2.16 & 0.75 \\ 2.16 & 1.29 & 0.48 \\ 0.75 & 0.48 & 0.21 \end{bmatrix} \\ \mathbf{k}^\top &= [0.70 \ 0.44 \ 0.20]. \end{aligned}$$

The prediction horizon is set to $N = 5$ and $\lambda = 1.1$. The resulting optimal control problem is solved in MATLAB using `fmincon`.

5.6 | Simulation Results

In the following we simulate the set point change from (u_0, y_0) to $(u_{\text{ref}}, y_{\text{ref}})$. We start by comparing the closed-loop results of the rGP-MPC, a batch GP approach (bGP-MPC), and an output

feedback MPC scheme (oMPC) that uses the model equations (16) and acts as a performance bound. We evaluate the performance for the three cases, where \mathcal{D}_0 , \mathcal{D}_{ref} , and $\mathcal{D}_{\text{comb}}$ are used as initial training data set. The bGP and rGP are initialized with the same initial training data and hyperparameters but the rGP updates its training data set during operation. We set $\bar{\sigma}^p = \bar{\sigma}^2 = 0$, such that every data point is considered as a candidate for inclusion⁹ with no upper limit on the number of data points. Hence, no points are removed. Due to the stochastic nature of the noise component, we simulate 50 times for each case. The results are depicted in Fig. 4 to Fig. 6. To quantify the performance we use the cost

$$V_{N_{\text{sim}}} = \sum_{k=0}^{N_{\text{sim}}} \ell(\mathbf{x}_k, u_k), \quad (18)$$

of the resulting state and input sequences, where N_{sim} is the number of total simulation steps. The results are presented in Tab. 3.

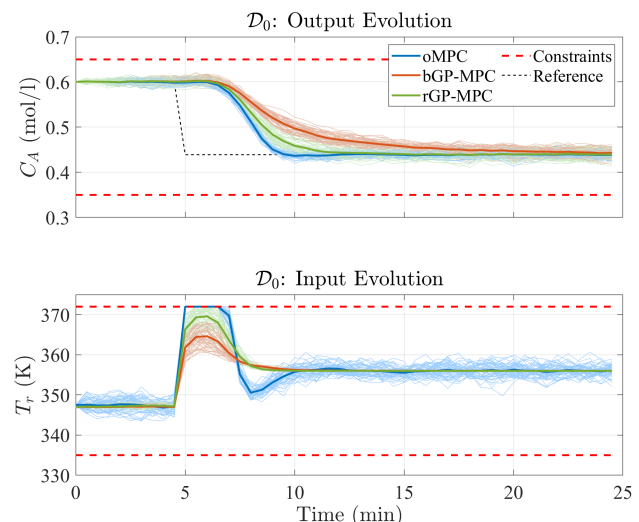


FIGURE 4 Comparison of the three MPC schemes for the case of initial training data \mathcal{D}_0 . Thin lines represent individual simulations, thick lines represent mean values.

As expected, the output MPC scheme that uses the true model performs best. The bGP has the worst performance in terms of larger settling time, though in terms of the performance measure it is in the $\mathcal{D}_{\text{comb}}$ case slightly better than the rGP because of the smaller input deviation. In the remaining cases, the performance of the rGP is better than that of the bGP due to the additional information gained during operation. The performance difference is especially large for \mathcal{D}_{ref} , where the

⁹Not every data point is added due to the update rule of Assumption 2.

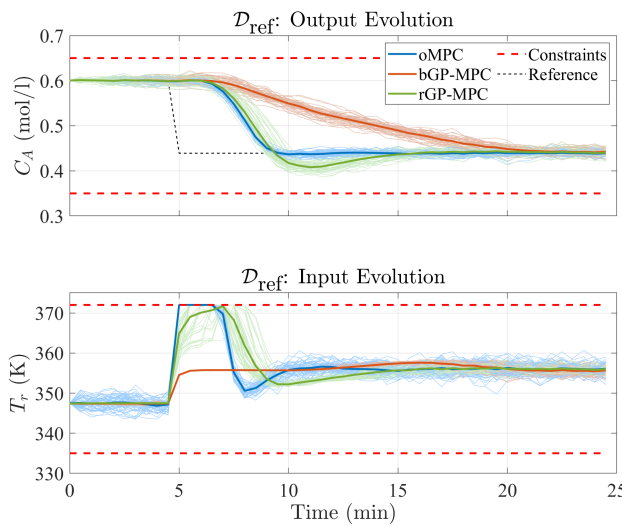


FIGURE 5 Comparison of the three MPC schemes for the case of initial training data \mathcal{D}_{ref} . Thin lines represent individual simulations, thick lines represent mean values.

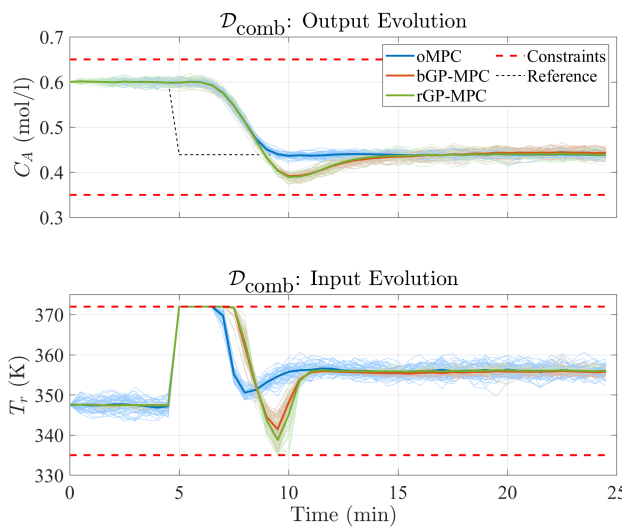


FIGURE 6 Comparison of the three MPC schemes for the case of initial training data $\mathcal{D}_{\text{comb}}$. Thin lines represent individual simulations, thick lines represent mean values.

bGP, throughout the whole operation, has only data points at the reference at its disposal but not at the initial condition. The rGP however performs significantly better due to the added data points, especially at the beginning of operation.

These simulations suggest that one should in general prefer the \mathcal{D}_{ref} case over the other cases, which is convenient for the used MPC scheme because knowledge at the reference is required anyway to determine the terminal cost and controller.

In the second set of simulations we investigate the influence of different thresholds for the data inclusion approach, i.e., different values for the maximum prediction error \bar{e}^p and the maximum prediction variance $\bar{\sigma}^2$. To this end, Fig. 7 combines the rGP results of the previous figures for the three training data cases, together with the evolution of the prediction error e^p and the prediction variance σ^2 . In particular the latter illustrates nicely the difference between the three cases. In the case of \mathcal{D}_0 , the variance is small at the beginning and increases around $t = 8$ min when the system leaves the neighborhood of the initial condition and moves towards the reference. The same holds, but the other way round, for the case with \mathcal{D}_{ref} , where the initial large error and variance is caused by their computation before the first data point is added to the training set.

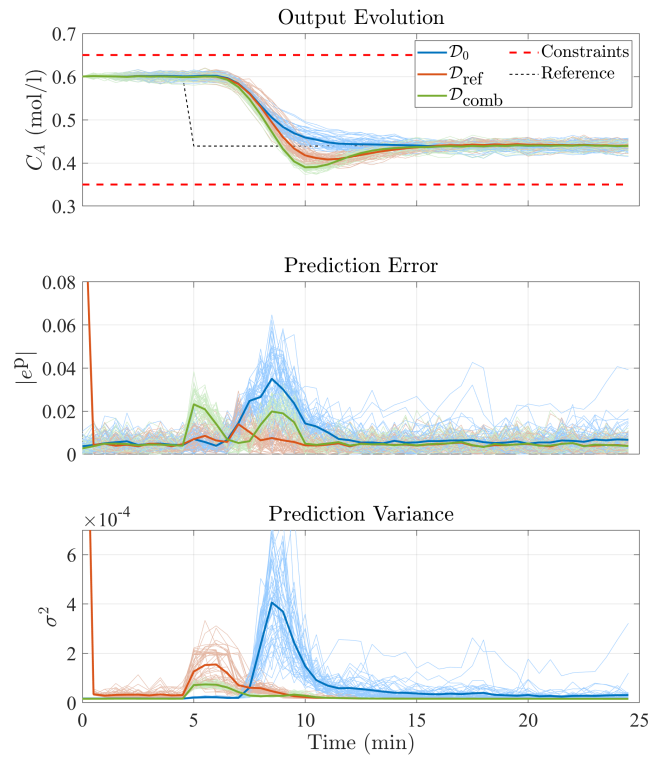


FIGURE 7 Simulation results with the rGP-MPC for the different training data cases together with the prediction error e^p and the prediction variance σ^2 .

Fig. 8 and Fig. 9 show results for different threshold values, where we focus for the sake of brevity on the simulation case with \mathcal{D}_{ref} . The results illustrate that instead of adding all data points, almost the same closed-loop performance can be achieved by adding only a fraction of them. Hence, this shows

not only that online learning can be achieved but also that it allows to work with significantly smaller training data sets, which in turn result in less computational costs.

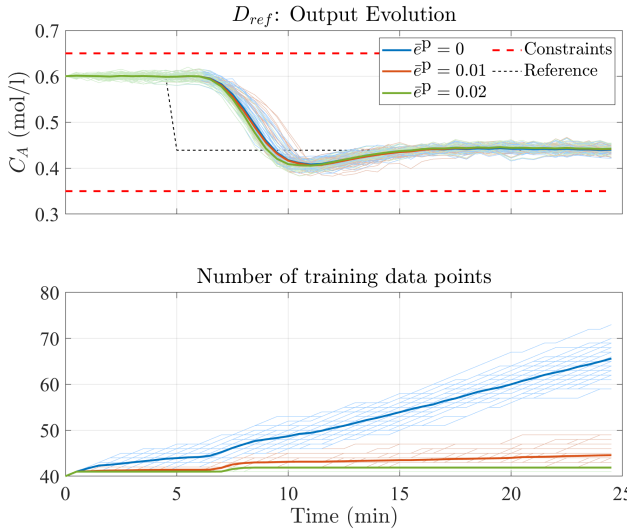


FIGURE 8 Influence of \bar{e}^p on the rGP-MPC with initial training data D_{ref} . With $\bar{e}^p = 0$, every encountered data point is considered to be added to the training data set. The variance threshold $\bar{\sigma}^2$ was set to a large value to not affect the result.

Next we consider the case that the number of training data points is limited by M . For the case of D_{ref} we set $M = 40$, which is the number of initially available training points, i.e., the training data set cannot increase but old data points are exchanged with newer more informative ones. To this end, whenever a new point is added, the oldest data point is removed. In Fig. 10 we compare the bGP (the initial training data set is not updated at all), the rGP with $M = \infty$, $\bar{e}^p = \bar{\sigma}^2 = 0$ (every encountered data point is considered to be added), and the rGP with $M = 40$, $\bar{e}^p = 0.01$, $\bar{\sigma}^2 = 2 \cdot 10^{-5}$ (data points are only exchanged). The bGP result is the same as in Fig. 5 and represents the worst case because the training data set is not updated at all. The $M = \infty$ case on the other hand represents the performance bound for this specific case because it includes the maximum of the incoming data points and does not remove any. Interestingly, the considered case of the rGP where data points are only exchanged performs basically as good as the performance bound, i.e., with a training data set of only 40 points, where the points are exchanged during operation, almost the same performance can be achieved as if every encountered point was included into the training data set D .

Besides the computational cost reduction due to the possibility to work with smaller training data sets, we illustrate at last the computational reduction due to the recursive update of

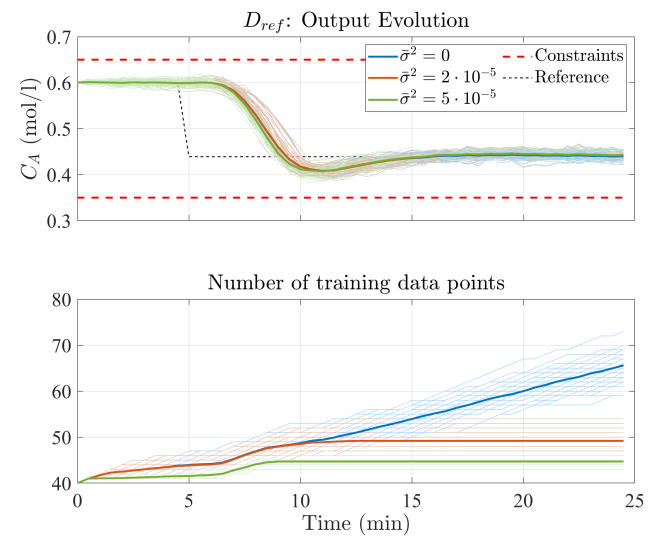


FIGURE 9 Influence of $\bar{\sigma}^2$ on the rGP-MPC with initial training data D_{ref} . With $\bar{\sigma}^2 = 0$, every encountered data point is considered to be added to the training data set. The prediction error threshold \bar{e}^p was set to a large value to not affect the result.

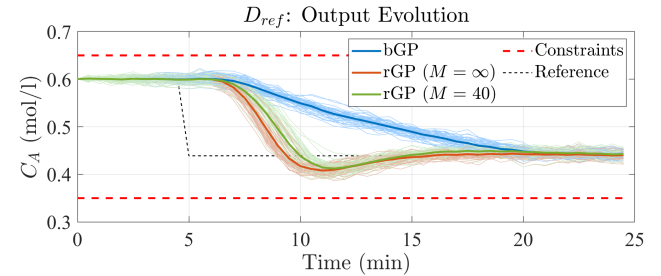


FIGURE 10 Influence of a limited number of training data points on the rGP-MPC with initial training data D_{ref} .

the Cholesky factor. In Fig. 11 we continue with the D_{ref} case, where we add every incoming point to the training data set and compare the computation times of the full and the recursive update of the Cholesky factor. The results show that the bigger the training data set becomes, the bigger the absolute and relative computational reduction. At $t = 24$ min the full recomputation of the Cholesky factor increases significantly. Investigations point to the reason lying in the generation of the covariance matrix and the inner workings of Matlab's `chol` function.

6 | CONCLUSION

We have presented a Gaussian process based nonlinear autoregressive model with exogenous input, employed as prediction

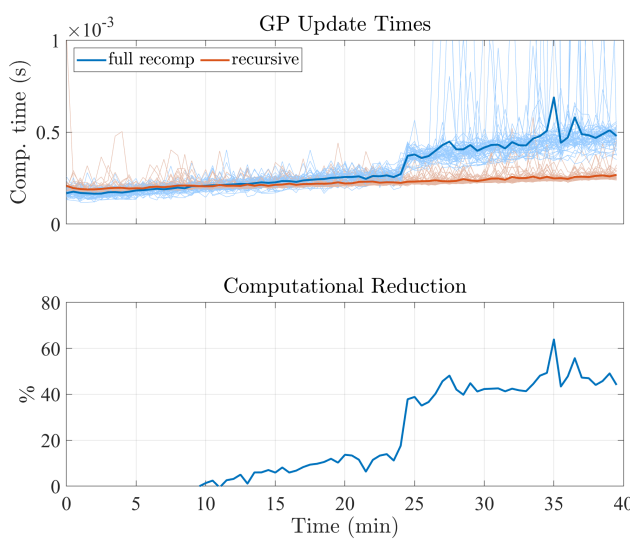


FIGURE 11 Comparison of computation times of the full recalculation of the Cholesky factor and the recursive update. The computational reduction that goes along with the recursive update increases with the amount of training data points.

model in an output feedback model predictive control scheme. The approach was extended to online learning, by means of updating the training data set, to account for limited a priori process knowledge. To this end, the concept of evolving GPs was adapted together with a recursive formulation to update the Cholesky decomposition to minimize computational cost. The resulting model predictive control scheme was shown to be input-to-state stable with respect to the process-model error, despite the time varying nature of the GP prediction model. In addition, the theoretic guarantees do not only apply to Gaussian processes but all online learning methods that satisfy the outlined conditions.

The approach was verified in different simulations, which have shown that it is in general possible to start with limited a priori process knowledge and refining the model along operation. One important finding is that it is particularly beneficial to start with a model that captures at least the behavior at the target reference, which is fortunately an intrinsic necessity for all MPC schemes that use a terminal/target region, cost, and controller to guarantee recursive feasibility and stability. Another finding was that the presented formulation yields good closed-loop performance with a quite small number of training data points, thereby efficiently reducing the computational load. This presents itself as a possible option for very fast processes, where hyperparameter optimization is not an option but some kind of online learning is desirable. Additionally, due to the output feedback scheme, this approach can be employed for processes, whose state cannot be measured or is difficult to be estimated.

Future work aims at implementing the presented approach in laboratory experiments, together with a combination of a deterministic base model and the Gaussian process prediction model. From a theoretical point of view, time varying reference tracking instead of set point changes would be interesting to investigate. For instance, what conditions does the initial training data set has to satisfy to achieve acceptable tracking results and how to automatically compute safe thresholds for the data inclusion approach. Another interesting question to investigate is how the approach performs for time varying processes. A hypothesis would be to combine the squared exponential covariance function with a non-stationary one to account for time variance in the process model.

References

1. Rawlings JB, Mayne DQ. *Model Predictive Control: Theory and Design*. Madison: Nob Hill Publishing . 2009.
2. Mayne DQ. Model Predictive Control: Recent Developments and Future Promise. *Automatica* 2014; 50(12): 2967–2986.
3. Lucia S, Kögel M, Zometa P, Quevedo DE, Findeisen R. Predictive Control, Embedded Cyberphysical Systems and Systems of Systems – A perspective. *Annual Reviews in Control* 2016; 41: 193–207.
4. Scokaert PO, Mayne D. Min-max Feedback Model Predictive Control for Constrained Linear Systems. *IEEE Transactions on Automatic Control* 1998; 43(8): 1136–1142.
5. Mayne DQ, Raković S, Findeisen R, Allgöwer F. Robust Output Feedback Model Predictive Control of Constrained Linear Systems. *Automatica* 2006; 42(7): 1217–1222.
6. Lucia S, Finkler T, Engell S. Multi-stage Nonlinear Model Predictive Control Applied to a Semi-batch Polymerization Reactor under Uncertainty. *Journal of Process Control* 2013; 23(9): 1306–1319.
7. Maiworm M, Bähge T, Findeisen R. Scenario-based Model Predictive Control: Recursive Feasibility and Stability. In: Proceedings of the 9th International Symposium on Advanced Control of Chemical Processes (ADCHEM). IFAC. ; 2015; Whistler, Canada: 50–56.
8. Paulson JA, Streif S, Findeisen R, Braatz RD, Mesbah A. Fast Stochastic Model Predictive Control of end-to-end Continuous Pharmaceutical Manufacturing. In: . 41 of *Computer Aided Chemical Engineering*. Elsevier. 2018 (pp. 353–378).

9. Ljung L. *System Identification (2nd Ed.): Theory for the User*. Upper Saddle River, NJ, USA: Prentice Hall PTR . 1999.
10. Yang X, Maciejowski JM. Fault Tolerant Control Using Gaussian Processes and Model Predictive Control. *International Journal of Applied Mathematics and Computer Science* 2015; 25(1): 133–148.
11. Ostafew CJ, Schoellig AP, Barfoot TD, Collier J. Learning-based Nonlinear Model Predictive Control to Improve Vision-based Mobile Robot Path Tracking. *Journal of Field Robotics* 2016; 33(1): 133–152.
12. Hewing L, Liniger A, Zeilinger MN. Cautious NMPC with Gaussian Process Dynamics for Autonomous Miniature Race Cars. In: European Control Conference (ECC). IEEE. ; 2018: 1341–1348.
13. Rasmussen CE, Williams CK. *Gaussian Processes for Machine Learning*. MIT press . 2006.
14. Kocijan J. *Modelling and Control of Dynamic Systems Using Gaussian Process Models*. Springer . 2016.
15. Kocijan J, Murray-Smith R, Rasmussen CE, Likar B. Predictive Control with Gaussian Process Models. In: The IEEE Region 8 EUROCON. Computer as a Tool. IEEE. ; 2003: 352–356.
16. Klenske ED, Zeilinger MN, Schölkopf B, Hennig P. Gaussian Process-based Predictive Control for Periodic Error Correction. *IEEE Transactions on Control Systems Technology* 2016; 24(1): 110–121.
17. Cao G, Lai EMK, Alam F. Gaussian Process Model Predictive Control of an Unmanned Quadrotor. *Journal of Intelligent & Robotic Systems* 2017; 88(1): 147–162.
18. Maiworm M, Limón D, Manzano JM, Findeisen R. Stability of Gaussian Process Learning Based Output Feedback Model Predictive Control. In: Conference on Nonlinear Model Predictive Control (NMPC). IFAC. ; 2018; Madison, USA: 551-557.
19. Ostafew CJ, Schoellig AP, Barfoot TD. Learning-based Nonlinear Model Predictive Control to Improve Vision-based Mobile Robot Path-tracking in Challenging Outdoor Environments. In: International Conference on Robotics and Automation (ICRA). IEEE. ; 2014: 4029–4036.
20. Hewing L, Zeilinger MN. Cautious Model Predictive Control using Gaussian Process Regression. *arXiv preprint arXiv:1705.10702* 2017.
21. Ortmann L, Shi D, Dassau E, Doyle FJ, Leonhardt S, Misgeld BJ. Gaussian Process-based Model Predictive Control of Blood Glucose for Patients with Type 1 Diabetes Mellitus. In: Asian Control Conference (ASCC). IEEE. ; 2017: 1092–1097.
22. Murray-Smith R, Sbarbaro D, Rasmussen CE, Girard A. Adaptive, Cautious, Predictive Control with Gaussian Process Priors. *IFAC Proceedings Volumes* 2003; 36(16): 1155–1160.
23. Kocijan J, Murray-Smith R. Nonlinear Predictive Control with a Gaussian Process Model. *Lecture Notes in Computer Science* 2005; 3355: 185–200.
24. Ažman K, Kocijan J. Non-linear Model Predictive Control for Models with Local Information and Uncertainties. *Transactions of the Institute of Measurement and Control* 2008; 30(5): 371–396.
25. Berkenkamp F, Moriconi R, Schoellig AP, Krause A. Safe Learning of Regions of Attraction for Uncertain, Nonlinear Systems with Gaussian Processes. In: Conference on Decision and Control (CDC). IEEE. ; 2016: 4661–4666.
26. Vinogradskaya J, Bischoff B, Nguyen-Tuong D, Romer A, Schmidt H, Peters J. Stability of Controllers for Gaussian Process Forward Models. In: International Conference on Machine Learning. PMLR. ; 2016; New York, USA: 545–554.
27. Akametalu AK, Kaynama S, Fisac JF, Zeilinger MN, Gillula JH, Tomlin CJ. Reachability-based Safe Learning with Gaussian Processes. In: Conference on Decision and Control (CDC). IEEE. ; 2014: 1424–1431.
28. Koller T, Berkenkamp F, Turchetta M, Krause A. Learning-based Model Predictive Control for Safe Exploration and Reinforcement Learning. *arXiv preprint arXiv:1803.08287* 2018.
29. Fisac JF, Akametalu AK, Zeilinger MN, Kaynama S, Gillula J, Tomlin CJ. A General Safety Framework for Learning-based Control in Uncertain Robotic Systems. *IEEE Transactions on Automatic Control* 2018.
30. Bethge J, Morabito B, Matschek J, Findeisen R. Multi-Mode Learning Supported Model Predictive Control with Guarantees. In: Proc. 6th Nonlinear Model Predictive Control Conf. (NMPC). IFAC. ; 2018: 616–621.
31. Aswani A, Gonzalez H, Sastry SS, Tomlin C. Provably Safe and Robust Learning-based Model Predictive Control. *Automatica* 2013; 49(5): 1216–1226.

32. Soloperto R, Müller MA, Trimpe S, Allgöwer F. Learning-Based Robust Model Predictive Control with State-Dependent Uncertainty. In: Conference on Nonlinear Model Predictive Control (NMPC). IFAC. ; 2018: 538–543.

33. Petelin D, Kocijan J. Control System with Evolving Gaussian Process Models. In: Workshop on Evolving and Adaptive Intelligent Systems (EAIS). IEEE. ; 2011: 178–184.

34. McKinnon CD, Schoellig AP. Learning Multimodal Models for Robot Dynamics Online with a Mixture of Gaussian Process Experts. In: International Conference on Robotics and Automation (ICRA). IEEE. ; 2017: 322–328.

35. Berkenkamp F, Turchetta M, Schoellig A, Krause A. Safe Model-based Reinforcement Learning with Stability Guarantees. In: International Conference on Neural Information Processing Systems. Curran Associates Inc. ; 2017: 908–918.

36. Maiworm M, Wagner C, Temirov R, Tautz FS, Findeisen R. Two-degree-of-freedom Control Combining Machine Learning and Extremum Seeking for Fast Scanning Quantum Dot Microscopy. In: American Control Conference (ACC). IEEE. ; 2018; Milwaukee, USA: 4360–4366.

37. Gregorčič G, Lightbody G. Gaussian Process Approach for Modelling of Nonlinear Systems. *Engineering Applications of Artificial Intelligence* 2009; 22(4-5): 522–533.

38. Roberts S, Osborne M, Ebdon M, Reece S, Gibson N, Aigrain S. Gaussian Processes for Time-series Modelling. *Philosophical Transactions of the Royal Society of London A: Mathematical, Physical and Engineering Sciences* 2013; 371(1984).

39. Yu H, Xie T, Paszczynski S, Wilamowski BM. Advantages of Radial Basis Function Networks for Dynamic System Design. *Transactions on Industrial Electronics* 2011; 58(12): 5438–5450.

40. Williams CK, Rasmussen CE. Gaussian Processes for Regression. In: Advances in Neural Information Processing Systems. MIT press. ; 1996: 514–520.

41. Kocijan J, Girard A, Banko B, Murray-Smith R. Dynamic Systems Identification with Gaussian Processes. *Mathematical and Computer Modelling of Dynamical Systems* 2005; 11(4): 411–424.

42. Ackermann ER, De Villiers JP, Cilliers P. Nonlinear Dynamic Systems Modeling Using Gaussian Processes: Predicting Ionospheric Total Electron Content over South Africa. *Journal of Geophysical Research: Space Physics* 2011; 116(A10).

43. Smola AJ, Bartlett PL. Sparse Greedy Gaussian Process Regression. In: Advances in Neural Information Processing Systems 13. MIT Press. 2001 (pp. 619–625).

44. Seeger M, Williams C, Lawrence N. Fast Forward Selection to Speed Up Sparse Gaussian Process Regression. *Artificial Intelligence and Statistics* 9 2003.

45. Neal RM. Monte Carlo Implementation of Gaussian Process Models for Bayesian Regression and Classification. *arXiv preprint physics/9701026* 1997.

46. Osborne MA. *Bayesian Gaussian Processes for Sequential Prediction, Optimisation and Quadrature*. PhD thesis. Oxford University, UK; 2010.

47. Van Vaerenbergh S, Lázaro-Gredilla M, Santamaría I. Kernel Recursive Least-squares Tracker for Time-varying Regression. *IEEE Transactions on Neural Networks and Learning Systems* 2012; 23(8): 1313–1326.

48. Pérez-Cruz F, Van Vaerenbergh S, Murillo-Fuentes JJ, Lázaro-Gredilla M, Santamaría I. Gaussian Processes for Nonlinear Signal Processing: An Overview of Recent Advances. *IEEE Signal Processing Magazine* 2013; 30(4): 40–50.

49. Limón D, Alamo T, Salas F, Camacho EF. On the Stability of Constrained MPC without Terminal Constraint. *IEEE Transactions on Automatic Control* 2006; 51(5): 832–836.

50. Manzano JM, Limón D, Muñoz de la Peña D, Calliess JP. Output Feedback MPC Based on Smoothed Projected Kinky Inference. *IET Control Theory & Applications* 2019; 13(6): 795–805.

51. Raković SV, Levine WS. *Handbook of Model Predictive Control*. Springer . 2019

52. Limón D, Alamo T, Raimondo D, et al. Input-to-state Stability: A Unifying Framework for Robust Model Predictive Control. In: Nonlinear Model Predictive Control. Springer. 2009 (pp. 1–26).

53. Abrahamsen P. *A Review of Gaussian Random Fields and Correlation Functions*. Norsk Regnesentral/Norwegian Computing Center Oslo . 1997.

54. De Nicolao G, Pillonetto G. A new Kernel-based Approach for System Identification. In: American Control Conference (ACC). IEEE. ; 2008: 4510–4516.

55. Pillonetto G, Chiuso A. Gaussian Processes for Wiener-Hammerstein System Identification. *IFAC Proceedings Volumes* 2009; 42(10): 838–843.

56. Seborg DE, Edgar TF, Mellichamp DA. *Process Dynamics and Control*. Wiley . 1989.

TABLE 1 CSTR Parameters

Param.	Explanation	Value
q_0	Reactive input flow	10 l/min
V	Liquid volume in the tank	150 l
k_0	Frequency constant	$6 \cdot 10^{10}$ 1/min
E/R	Arrhenius constant	9750 K
ΔH_r	Reaction enthalpy	10000 J/mol
UA	Heat transfer coefficient	70000 J/(min K)
ρ	Density	1100 g/l
C_p	Specific heat	0.3 J/(g K)
τ	Time constant	1.5 min
C_{Af}	C_A in the input flow	1 mol/l
T_f	Input flow temperature	370 K

TABLE 2 Hyperparameters

	c	l_1	l_2	l_3	l_4	σ_f^2
D_0	0.64	0.07	0.38	0.14	6.43	0.05
D_{ref}	0.38	0.12	6.28	0.32	2.60	0.07
D_{comb}	0.50	0.52	1.76	1.11	1.25	0.30

TABLE 3 MPC Performance computed by (18).

	D_0	D_{ref}	D_{comb}
oMPC	59.4	59.4	59.4
bGP-MPC	69.7	89.8	62.4
rGP-MPC	62.0	62.1	63.8

How to cite this article: Maiworm M., D. Limon, and R. Find-eisen (2020), Online Gaussian Process learning-based Model Predictive Control with Stability Guarantees, *International Journal of Robust and Nonlinear Control*, **2020;00:1–6**.

Algorithm 1 Recursive Gaussian Process Model Predictive Control

MPC Parameters: Prediction horizon N , stage cost $\ell(\cdot)$ with respective parameters, hard input constraint set \mathcal{U} , soft output constraint set \mathcal{Y} .

rGP Parameters: Prior mean $m(\cdot)$, covariance function $k(\cdot, \cdot)$, initial hyperparameters θ , thresholds \bar{e}^p and $\bar{\sigma}^2$, maximum number of training points M .

Initialization

Training data set \mathcal{D} .

Optimize hyperparameters θ (7) with initial data set \mathcal{D} .

Initialize GP posterior mean function $m_+(\mathbf{w})$ with covariance matrix \mathbf{K} , Cholesky factor \mathbf{R} , and α (Sec. 3.3).

Compute GP posterior mean gradient $\nabla m_+(\mathbf{w})$ (Sec. 4.3).

Compute linear GP model at \mathbf{x}_{ref} (Sec. 5.5).

Compute terminal cost function $V_f(\cdot)$ (Sec. 5.5).

Recursion

for each time step k **do**

Solve optimal control problem (14) for initial condition \mathbf{x}_k and obtain optimal input sequence $\hat{\mathbf{u}}_{k|k}^*$.

Apply first element $u_k = \kappa_{MPC}(\mathbf{x}_k | \mathcal{D}_k) = \hat{\mathbf{u}}_{k|k}^*$.

Simulate system response and get new output y_{k+1} .

Construct new GP data point $S_{k+1} = (\mathbf{w}_k, z_k)$ with $\mathbf{w}_k = (\mathbf{x}_k, u_k)$ and $z_k = y_{k+1}$.

Update GP:

Compute $\hat{y}_{k+1} = m_+(\mathbf{w}_k | \mathcal{D}_k)$ and $\sigma_+^2 = \sigma_+^2(\mathbf{w}_k | \mathcal{D}_k)$.

if $|y_{k+1} - \hat{y}_{k+1}| > \bar{e}^p$ OR $\sigma_+^2 > \bar{\sigma}^2$ **then**

$\mathcal{D}'_{k+1} = \mathcal{D}_k \cup S_{k+1}$.

Using \mathcal{D}'_{k+1} update \mathbf{K} and \mathbf{R} via (10).

if number of training points $> M$ **then**

Remove oldest data point and downdate \mathbf{K} and \mathbf{R} via (11).

end if

Recompute α .

end if

if $V_N^*(\mathbf{x}_k | \mathcal{D}'_{k+1}) \leq V_N^*(\mathbf{x}_k | \mathcal{D}_k)$ **then**

$\mathcal{D}_{k+1} \leftarrow \mathcal{D}'_{k+1}$

else

$\mathcal{D}_{k+1} \leftarrow \mathcal{D}_k$

end if

end for